Rapid circulation of warm subtropical waters in a major glacial fjord in East Greenland

Fiammetta Straneo[1], Gordon S. Hamilton[2], David A. Sutherland[1*], Leigh A. Stearns[2†], Fraser Davidson[3] , Mike O. Hammill[4], Garry B. Stenson[3] and Aqqalu Rosing-Asvid[5]

[1] *Department of Physical Oceanography, Woods Hole Oceanographic Institution, Woods Hole, MA 02543, USA*

[2] *Climate Change Institute, University of Maine, Orono, ME 04469, USA*

[3] *Department of Fisheries and Oceans, St. John's, Newfoundland, A1C 5X1, Canada*

[4] *Department of Fisheries and Oceans, Mont-Joli, Quebec, G5H 3Z4, Canada*

[5] *Department of Birds and Mammals, Greenland Institute of Natural Resources, Postboks 570, 3900 Nuuk, Greenland.*

---

* Present address: School of Oceanography, University of Washington, Seattle, WA 98195

† Present address: Department of Geology, University of Kansas, Lawrence, KS 66045, USA

The recent rapid increase in mass loss from the Greenland Ice Sheet[1,2] is primarily attributed to an acceleration of outlet glaciers[3-5]. One possible cause is increased melting at the ice/ocean interface[6,7] driven by the synchronous warming[8-10] of subtropical waters offshore of Greenland. This hypothesis is largely untested, however, because of the lack of observations from Greenland's glacial fjords and our limited understanding of their dynamics. Here, we present new ship-based and moored oceanographic data, collected in Sermilik Fjord, a large glacial fjord in East Greenland, showing that subtropical waters are present throughout the fjord and are continuously replenished via a wind-driven exchange with the shelf, where they occur year-round. The temperature and rapid renewal of these waters suggest that, at present, they drive enhanced submarine melting at the terminus. Key controls on the melting rate are the volume and properties of subtropical waters on the shelf and the patterns of the along-shore winds, suggesting the glaciers' acceleration was triggered by a combination of atmospheric and oceanic changes. These measurements provide evidence of rapid advective pathway for the transmission of oceanic variability to the ice-sheet margins and highlight an important process that is missing from prognostic ice-sheet models.

The Greenland Ice Sheet's contribution to sea level rise more than doubled in the last decade[1,2], predominantly due to the acceleration of outlet glaciers flowing into deep fjords in western and southeastern Greenland[3,4,5]. The glacier speed-up occurred approximately at the same time as a warming trend began in the subpolar North Atlantic Ocean, adjacent to Greenland's southeastern and western sectors[8-10], giving rise to the hypothesis that glacier acceleration was triggered by ocean warming[11-13]. The proposed mechanism involves enhanced melting at the front of the glacier, driven by increased ocean heat transport, which leads to ice thinning, ungrounding of the terminus and ice flow acceleration[6,7].

A lack of measurements from Greenland's glacial fjords, however, makes it difficult to test this hypothesis. First, the warming waters belong to the Irminger Current (IC), a topographically-steered branch of the North Atlantic Current (NAC), which carries warm, subtropical water (STW) into the subpolar basin (Figure 1a). This water is trapped offshore over the continental slope, while cold, fresh polar water (PW), transported by the East and West Greenland Currents (EGC and WGC; Figure 1a) dominates the shelf adjacent to the fjords[14]. Evidence that STW reaches Greenland's fjords is limited to a few summer profiles from Jakobshavn[12] and Kangerdlugssuaq[15] fjords and there is no direct evidence that it comes into contact with glaciers. The lack of adequate fjord measurements from the period prior to the glaciers' acceleration, in particular, means that we need to rely on our understanding of the processes which control the properties and circulation within the fjords (and hence the heat transport to the glaciers' termini) in order to infer past conditions and assess the ocean's role in triggering the acceleration of Greenland's glaciers. At present, the mechanisms governing the circulation of STW on the shelf and inside Greenland's glacial fjords are unknown.

The 100 km long Sermilik Fjord (66º N, 38º W) connects Helheim Glacier with the Irminger Sea (Figure 1b). In 2003, Helheim Glacier retreated several kilometers and almost doubled its flow speed[3,4]. Warm STW has recently been observed outside the fjord on the shelf[16] but there are no records of ocean properties within the fjord itself. We collected thirty-eight temperature and salinity profiles, together with bathymetric and current data, in and just offshore of Sermilik Fjord during two surveys in July and September, 2008 (Figure 1b). Additional data were collected by several moored instruments (Figure 1b; see Methods Summary).

Sermilik is a U-shaped glacial trough which is deeper (900 m at the mouth) than most of the adjacent shelf (300-400 m). No sill was found in our surveys. Instead we identified a 700 m deep channel extending from the mouth (Figure 1b) towards a deep trough that stretches across the entire shelf (Figure 1a). In September, this 20 km wide channel was mostly filled with warm (4.2 ºC) STW which, assuming geostrophy and no flow at the bottom, was flowing towards the fjord. Slightly cooler STW (3.5-4 ºC) was present in large volumes inside the fjord from a depth of 200-300 m to the bottom at all surveyed locations (Figure 2 a-c). A 10-20 m thick layer of glacial meltwater (GM) and a 100-150 m thick layer of PW were found above STW throughout the fjord (Figure 2 a-c).

Property changes within the fjord were mostly in the along-fjord direction with limited across-fjord variation (consistent with a narrow fjord not strongly influenced by rotation).

The same three water masses were present in the fjord during both surveys but with different characteristics in the upper 300-400 m (Figure 2). In particular, the PW layer was noticeably thinner and warmer in September, which increased the mean temperature of the upper 400 m from 0.5 to 2 ºC. This warming is too large to be driven by local heating (it requires a surface heat flux of 470 W/m^2 for July and August which is three times larger than that estimated for the same period from the National Center for Environmental Prediction Renalysis[17] for the region outside the fjord, shown in Figure 3c) and, also, surface fluxes would not penetrate deep in this highly stratified environment. Thus, the change must result from the advection of warmer waters into the fjord, as confirmed by the presence of different water masses in the upper layers in July and in September (Figure 2a-c). To investigate whether changes in the fjord are consistent with those occurring outside the fjord, we reconstructed the seasonal variation of temperature on the shelf using data collected by 19 Hooded seals (*Cystophora cristata*) tagged with satellite-linked temperature-depth recorders[18] (5269 dives from 2004 to 2008[19]) (Figure 3). These data reveal that STW (subsurface waters warmer than 3.5 ºC) are present on the shelf year round and, also, that the shelf waters warm from July to December. Both the trend and the magnitude of the warming (the shelf's upper 400 m also warm by ~1.5 ºC from July to September) support the conclusion that changes in the fjord are a result of advection from the shelf. (The shelf temperatures are warmer than those in the fjord because they represent a spatial average across the shelf, including regions close to undiluted STW on the slope.)

The rapid flushing of the upper waters of the fjord indicates a vigorous circulation. We investigate its nature by first considering an estuarine-type circulation, driven by a large melt water input at the head, consisting of a fresh outflow at the surface balanced by a saltier, subsurface inflow (see Supplementary Figure 1a). The magnitude of the estuarine circulation and the related flushing time are estimated from the observed vertical property distribution and by applying conservation of mass and salt. Assuming the circulation is limited to the upper 300 m, the 'fastest' estimated flushing time is ~2 years (see Supplementary Methods), indicating that the observed summertime changes cannot be attributed to this type of circulation alone.

A second type of circulation common in narrow, deep fjords[20] is an 'intermediary circulation'[21] driven by pressure gradients which arise between the fjord and the coastal region. It is associated with strongly sheared flows and an exchange of properties that persist until the fjord (the smaller volume) has equilibrated to the coastal region. Several pieces of evidence indicate that such a circulation may dominate in Sermilik Fjord. First, we observed large, strongly-sheared currents in the upper 100-200 m during both surveys (Figure 2e and g). These currents are more vigorous than the expected 10-15 cm/s tidal currents, which would arise from a barotropic tide in a 800 m deep channel and a tidal range of 1.5 m (the maximum range measured by a tide-gauge deployed in the fjord from

July-September 2008). Second, the observed currents must, by continuity, have compensating outgoing currents at depth, otherwise they would raise sea-level in the fjord by several meters within one hour which is inconsistent with the tide-gauge data.

Intermediary circulations can be driven by any forcing which results in fjord/shelf gradients[20] but our observations indicate along-shore winds as the dominant driver in Sermilik Fjord. Northeasterly wind events, for example, will initially 'pile-up' water and depress the halocline at the mouth of the fjord driving an inflow in the upper layer and at outflow at depth which, in turn, raises sea-level and depresses the halocline in the fjord. Once the winds subside, and the shelf relaxes back to the pre-event state, the fjord responds with the reverse circulation pattern (see Supplementary Figure 1).

Several along-shore wind events, which occurred during our surveys and mooring occupations, allow us to test the wind-driven intermediary-circulation hypothesis. Both surveys were conducted during or immediately after strong northeasterly (see Figure 3c for direction) wind events (Figure 4a) and the observed velocities and shear are consistent with the expected response. Clear evidence for depression of the halocline at the mouth of the fjord (Figure 2d) was found in the first survey, which took place during a wind event. Assuming the observed velocities were sustained, the upper 300 m of the fjord would be renewed within 4 days. Also, data collected by two summer moorings (see Figure 1b for location, and Methods Summary for a description) show qualitatively that northeasterly wind events are associated with a temporary downward displacement (by

50-100 m) of the isotherms (Figure 4b) and a temporary freshening at 25 m and 180-200 m (Figure 4c), consistent with the response described above. While the summer mooring records are too short to establish statistical significance, an 8 month record of pressure, temperature and salinity from a third mooring reveals that anomalies in all three fields are significantly correlated with along-shore wind events, and of the sign expected for a wind-forced intermediary circulation (see Supplementary Figure 2). We conclude that along-shore wind events, which are intense and frequent along Greenland's eastern coast[22], control the renewal rate of waters in Sermilik Fjord and cause the fjord to track sub-seasonal changes on the shelf.

The presence of large volumes of STW in Sermilik Fjord during the summer, their renewal rate and observations that these waters are found on the shelf year-round, suggest that STW are also present in the fjord year-round. Their temperature, circulation and along-fjord retention of heat indicate that significant submarine melting is occurring at Helheim Glacier, which has an estimated terminus depth of 700 m[23]. Key controls to the rate of melting are the volume and properties of STW on the shelf as well as the along-shore winds. Since the characteristics of Sermilik Fjord and of the nearby shelf/slope region, including the along-shore winds[22] and deep channels[24] stretching across the shelf, are common to glacial fjords in southeastern and western Greenland, it is likely that these results can be generalized to other glacial fjords in this region – which contains the majority of the accelerating glaciers[1].

The data presented here are limited to the period that followed Greenland's glaciers' accelerations and, thus, cannot provide direct evidence on the ocean's role in triggering the acceleration. Nonetheless, our results offer several new insights to this issue. First, the presence and renewal of STW in Sermilik Fjord provides evidence of a fast and direct pathway connecting the subpolar North Atlantic Ocean to glacial fjords along Greenland's southeast and west coasts. This supports the proposed hypothesis that changes in the North Atlantic might have impacted Greenland's glaciers within one year[12]. Second, our findings indicate that either changes in the volume and properties of STW on the shelf and/or changes in the intensity and number of transiting storms[25] would affect melting at the tidewater margins of outlet glaciers. Both mechanisms are plausible (and likely connected) given the pronounced changes in the N. Atlantic's ocean and atmosphere which began in the mid-1990s[26,27]. Thus, our findings support increased submarine melting as a trigger for the glacier acceleration but indicate a combination of atmospheric and oceanic changes as the likely driver.

Methods Summary

Measurements in Sermilik Fjord were conducted from a locally-chartered 24 foot vessel. Conductivity, temperature and depth (CTD) profiles were collected using a 6 Hz XR-620 RBR sensor to 800 m in July and to 600 m in September. Four to six CTD profiles were collected across sections 1, 2, 3 and one at station A between July 4-6 and again between August 31-September 3, when sections S and 4 (Figure 1b) were added. Cross-instrument and pre- and post-deployment calibrations were carried out. Underway velocity data were collected using a vessel-mounted 300 kHz RDI Acoustic Doppler Current Profiler, combined with continuous vessel tracking by Global Position System, across section 2 in July and across sections 2 and 3 in September. Bathymetric data were obtained using a 320 Knudsen 12 kHz Echosounder.

Two moorings were deployed at depths of 25 and 180 m from July to September and a third mooring was deployed at 35 m from September 2008 to August 2009 (Figure 1b). All three moorings carried a Seabird SBE 37-SM CTD recorder approximately 1 m above the bottom. In addition, the deeper mooring carried a thermistor string consisting of 10 Starmon Mini Temperature Recorders, spaced 10 m apart from the bottom to 100 m off the bottom. An RBR DR1050 depth recorder located above the uppermost recorder provided a measure of mooring tilt. The deep mooring was hit by ice three times and eventually displaced to a depth of 220m. The 35 m mooring was also hit by ice and displaced several times until it settled at 65 m at the end of December (where it stayed until it was recovered). All three moorings were located within 300 m of each other and displacements were less than 100 m.

1. Rignot, E. & Kanagaratnam, P. Changes in the velocity structure of the Greenland Ice Sheet. *Science* **311,** 986-990 (2006).

2. Velicogna, I. Increasing rates of ice mass loss from the Greenland and Antarctic ice sheets revealed by GRACE. *Geophys. Res. Lett.* **36**, doi:10.1029/2009GL040222 (2009).

3. Stearns, L. A. & Hamilton, G. S. Rapid volume loss from two East Greenland outlet glaciers quantified using repeat stereo satellite imagery. *Geophys. Res. Lett.* **34,** L05503, doi:10.1029/2006GL028982 (2007).

4. Howat, I. M., Joughin, I. & Scambos, T.A. Rapid changes in ice discharge from Greenland Outlet Glaciers. *Science* **315,** 1559-1561 (2007).

5. Joughin, I., Abdalati, W. & Fahnestock, M. Large fluctuations in speed on Greenland's Jakobshavn Isbræ glacier. *Nature* **432**, 608-610 (2004).

6. Thomas, R. H. Force-perturbation analysis of recent thinning and acceleration of Jakobshavn Isbræ, Greenland *J. Glaciol*. **50**, 57-66 (2004).

7. Nick, F. M., Vieli, A., Howat, I., M. & Joughin, I. Large-scale changes in Greenland outlet glacier dynamics triggered at the terminus. *Nature Geosci.* **2,** 110-114 (2009).

8. Myers, P. G., Kulan, N. & Ribergaard, M. H. Irminger Water variability in the West Greenland Current. *Geophys. Res. Lett*. **34**, L17601, doi:10.1029/2007GL030419 (2007).

9. Bersch, M., Yashayaev, I. & Koltermann, K. P. Recent changes of the thermohaline circulation in the Subpolar North Atlantic. *Ocean Dyn*. **57**, 223-235 (2007).

10. Thierry, V., de Boisséson, E. & Mercier, H. Interannual variability of the Subpolar Mode Water properties over the Rejkyanes Ridge during 1990-2006. *J. Geophys. Res*. **113**, C04016, doi:10.1029/2007JC00443 (2008).

11. Bindschadler, R. Hitting the ice sheet where it hurts, *Science* **311** 1720-1721 (2006).

12. Holland, D. M., Thomas, R. H., De Young, B., Ribergaard, M. H. & Lyberth, B. Acceleration of Jakboshavn Isbræ triggered by warm subsurface ocean waters. *Nature Geosci.* **1**, 659-664 (2008).

13. Hanna, E. *et al*. Hydrologic response of the Greenland ice sheet: the role of oceanographic warming *Hydrol. Process.* **23**, 7-30 (2009).

14. Bacon, S., Myers, P. G., Rudels, B. & Sutherland, D. A. Accessing the inaccessible: Buoyancy-driven coastal currents on the shelves of Greenland and Eastern Canada. *Arctic-Subarctic Ocean Fluxes: Defining the role of the Northern Seas in Climate: Eds. R. Dickson, J. Meincke, P. Rhines, Springer-Verlag, NY, pp740,* (2008)

15. Azetsu-Scott, K. & Tan, F. C. Oxygen isotope studies from Iceland to an East Greenland Fjord: behaviour of glacial meltwater plume. *Marine Chem.* **56**, 239-251 (1997).

16. Sutherland, D. A. & Pickart, R. S. The East Greenland Coastal Current: Structure, variability, and forcing. *Prog. Oceanogr.* **78**, 58-77 (2008).

17. Kalnay, E., et al. The NMC/NCAR 40-Year Reanalysis Project. *Bull. Amer. Meteor. Soc.*, **77**, 437-471 (1996).

18. Lydersen, C., Nøst, O. A., Kovacs, K. M. & Fedak, M. A. Temperature data from Norwegian and Russian Waters of the northern Barents Sea collected by free-living ringed seas. *J. Mar. Systems* **46**, 99-108 (2004).

19. Andersen, J. M., Wiersma, Y. F. & Stenson, G. B., Hammill, M. O. & Rosing-Asvid, A. Movement patterns of Hooded seals (*Cystophora cristata*) in the Northwest Atlantic Ocean during the post-moult and pre-breed seasons. *J. Northw. Atl. Fish. Sci. (in press).*

20. Klinck, J. M., O’Brien, J. J. & Svendsen, H. A simple model of fjord and coastal circulation interaction. *J. Phys. Ocean*. **11**, 1612-1626 (1981).

21. Stigebrandt, A. On the response of the horizontal mean vertical density distribution in a fjord to low-frequency density fluctuations in the coastal water. *Tellus* **42A** 605-614 (1990).

22. Moore, G. W. K. & Renfrew, I. A. Tip jets and barrier winds: A QuickSCAT climatology of high wind speed events around Greenland. *J. Climate* **18**, 3713-3725 (2005).

23. Thomas, R. *et al.* Substantial thinning of a major east Greenland outlet glacier. *Geophys. Res. Lett.* **27**(9), 1291-1295 (2000).

24. Roberts, D. H., Long, A. J., Schnabel, C., Freeman, S. & Simpson, M. J. R. The deglacial history of southeast sector of the Greenland Ice Sheet during the Last Glacial Maximum. *Quat. Sci. Rev.* **27**, 1505-1516 (2008).

25. Aure, J., Molvær, J. & Stigebrandt, A. Observations of inshore water exchange forced by a fluctuating offshore density field. *Mar. Pollut. Bull.* **33**, 112-119 (1997).

26. Häkkinen, S. & Rhines, P. B. Decline of Subpolar North Atlantic Circulation during the 1990s. *Science* **304**, 555-559 (2004).

27. Häkkinen, S. & Rhines, P. B. Shifting surface currents in the northern North Atlantic Ocean. *J. Geophys. Res.* **114**, doi:10.1029/2008JC004883 (2009).

Supplementary Information accompanies the paper on **www.nature.com/nature**.

Acknowledgements We thank J, Ryder and A. Jorgensen for support in the field work; J. Kemp for logistic support, D. Torres, K. Newhall, S. Worrilow and A. Newhall for instrument preparation; R.S. Pickart. S. Lentz and R. Curry for instructive discussions, and Greenpeace International and the crew of the Arctic Sunrise for support in 2009 mooring recovery. F.S. acknowledges support from WHOI's Ocean and Climate Change Institute's Arctic Research Initiative and from NSF OCE 0751896, and G.S.H and L.A.S from NASA's Cryospheric Sciences Program. Funding for the hooded seal deployments was obtained from the International Governance and Atlantic Seal Research Program, Fisheries and Oceans, Canada, to G. B. S. and to the Greenland Institute of Natural Resources to A. R. A.

Authors' Contributions FS and GSH conceived the study, F.S., D. A. S., L. A. S. and G. S. H. participated in the collection of oceanographic data in Sermilik Fjord, and F.S. and D. A. S. were responsible for the analysis. M. O. H., G. B. S. and A. R. A. were responsible for the capture of the seals and deployment of the transmitter and F.D. for processing the data from the seals. .

Author Information Correspondence and requests for materials should be addressed to F.S. (fstraneo@whoi.edu).

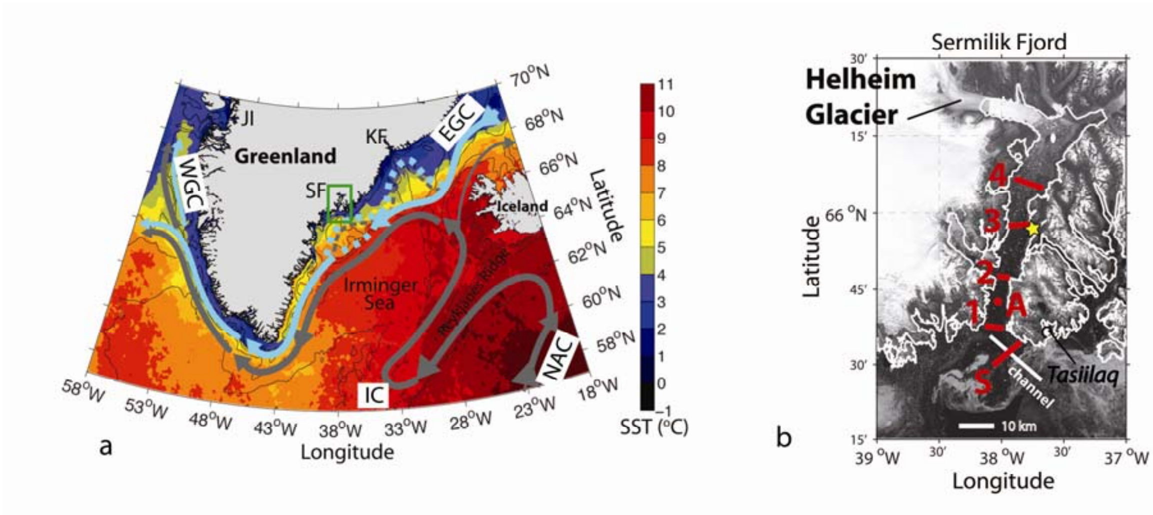

Figure 1 a) Currents around Greenland overlaid on the 2003 mean sea-surface temperature from the Advanced Very High Resolution Radiometer (filled contours). Bathymetric contours (100, 500, 1000, 2000, 3000 m) are overlaid in black. PW transported by the EGC and WGC is in blue (dashed paths indicate multiple branches) and STW transported by the NAC and IC in gray. Sermilik Fjord (SF, green box), Kangerdlugssuaq Fjord (KF) and Jakobshavn Isbrae (JI) are indicated. b) Landsat mosaic of Sermilik Fjord. Sections (1-4, S) plus station A occupied in the 2008 surveys are indicated in red, moorings' locations by the yellow star.

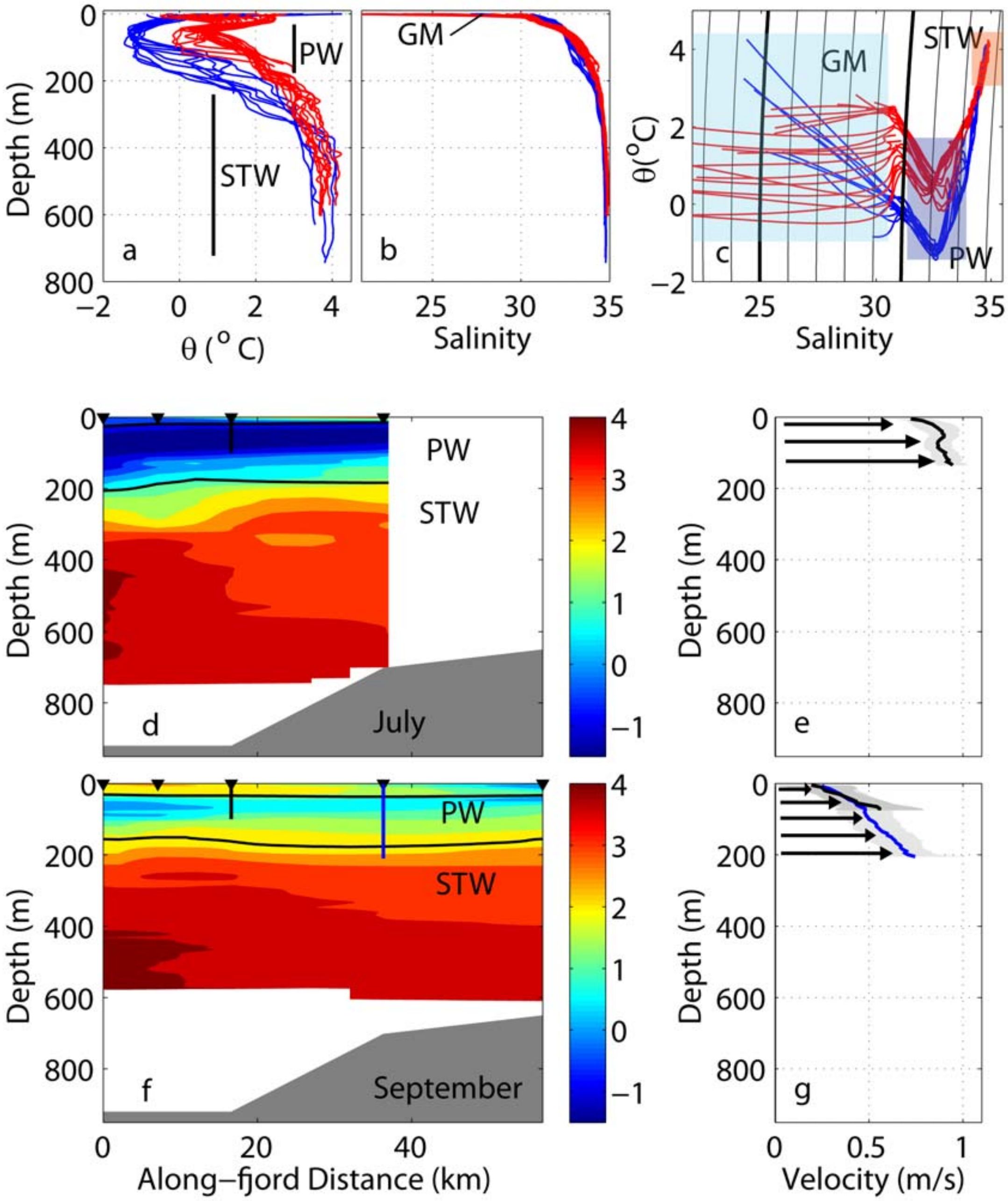

Figure 2. Measurements in Sermilik Fjord in summer 2008 and the 3 watermasses, GM, PW and STW. **a)** Potential temperature in July (blue) and

September (red); **b)** Salinity (colors as a). **c)** Potential temperature versus salinity (colors as a). Potential density contours are overlaid in black (thick lines are σ_θ=20 and 25 kg/m^3) **d)** and **f)** Potential temperature distribution in the along-fjord direction (x=0 is the mouth) from across-section averages, in July and September, respectively. The 31.5 and 34 isohalines are overlaid to separate the 3 layers. Top triangles indicate section location and vertical bars the velocity sections. Bathymetry is shaded in gray. **e**) and **g**) Along-fjord velocity averaged across-fjord at the sections indicated in d) and f) respectively, positive is towards the head of the fjord. Shading indicates the standard deviation across the section; arrows indicate direction of flow.

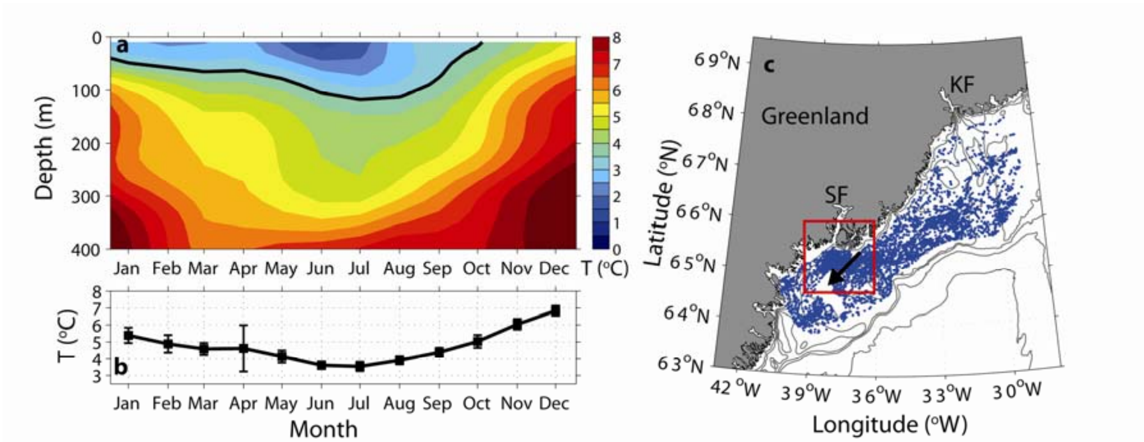

Figure 3 Seasonal temperature variation on the East Greenland Shelf from tagged Hooded seals. a) monthly and spatially averaged temperature profiles versus depth (solid line is 3.5ºC and approximately separates the PW from the STW). b) mean monthly temperature averaged over the upper 400m (vertical bars indicate standard error). c) locations of the 5269 seal dives. Both the winds and the heat fluxes referred to in the text were averaged over the red box shown. The direction of the northeasterly winds (oriented at 54º) is shown by the black arrow.

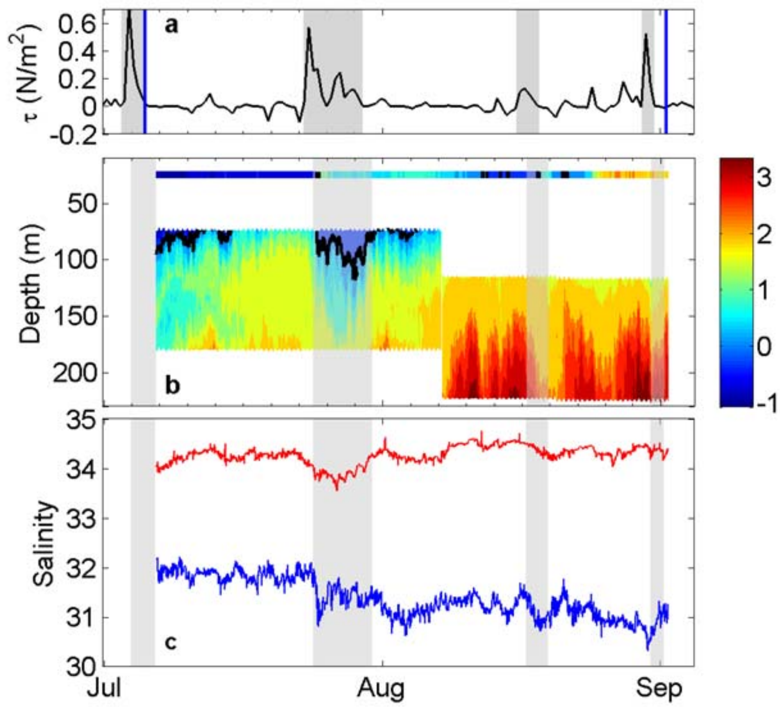

Figure 4. Along-shore winds in Sermilik Fjord. a) Northeasterly wind stress outside of Sermilik Fjord from Quikscat. Wind events are shaded (see Supplementary Methods). Blue lines show when the velocity data was collected. b) Potential temperature from the two summer moorings. Data from the 11 temperature recorders was vertically interpolated. The deep mooring was hit by ice and relocated 40 m deeper in early August. Wind-events as in a) but lagged by one day (see Supplementary Methods) c) Salinity from the two moorings at 25 m (blue) and at 180-200 m (red). Shaded regions as in b).

Supplementary Methods

Estuarine Circulation

We estimate the magnitude of the estuarine circulation in the fjord by assuming a simple two-layer system with an outflowing fresh plume and an inflowing saltier layer (Supplementary Figure 1a). Using relations for the conservation of mass and salt[28], the fjord's flushing time (T_f) due to an estuarine circulation is:

$$T_f = \frac{(h_{out} + h_{in})WL}{S_{in}R}(S_{in} - S_{out}),$$

where W is the width of the fjord (8 km), L the length (100 km), R the rate of melt water input, h the layer thickness, S the salinity, and subscripts '*in*/*out*' refer to the inflowing deep, salty layer and the outflowing fresh layer, respectively. If we assume the estuarine circulation is confined to the upper 300m (the layer over which we observed the most pronounced changes), data from the two surveys yield the following estimates: h_{out} ~ 10-20 m, h_{in} ~ 280m, S_{in} ~ 33-33.3, S_{out} ~ 28-29.5.

To estimate meltwater input, R, we first consider Helheim Glacier, the dominant source of meltwater for Sermilik Fjord. Measurements of exposed stake heights on Helheim Glacier (GSH and LAS, unpublished data) yield surface melt rates of ~4 m/yr at 100 m asl and ~2 m/yr at 700 asl. We use a simple linear scaling to apply these estimates to the glacierized area surrounding the upper portion of Sermilik Fjord using a digital elevation model[3] to obtain a liquid water runoff of ~5 Gt/yr. An unknown amount of liquid water is generated by submarine melting at the tidewater terminus of Helheim Glacier and by icebergs in the fjord which, for the purposes of this calculation, we assume is equal to the terrestrial runoff. This yields a net value for *R* (~10 Gt/yr) which is probably an underestimate because we neglected 1) snow-melt runoff from the non-glacierized land-surface and 2) meltwater from other portions of the ice sheet bordering the fjord as well as local glaciers. To account for this and, in general, to minimize the flushing time estimate, we more than double our estimated fresh water input and use *R*~ 25 Gt/yr = 25 km^3/yr.

Using these values, the estimated flushing time of the upper 300 m is > 2 yr, with a mean inflow velocity of 0.1 cm/s and an outflow velocity of 2 cm/s. It would take more than 5 years to flush the entire fjord (assuming a mean depth of 700 m). We emphasize that the purpose of this simple calculation is to maximize the magnitude of the estuarine circulation (and minimize the flushing time); even taking the maximum range of input values yields a flushing time that is an order of magnitude slower than that implied from our field observations. This suggests that, while still contributing to the net circulation within the fjord, the meltwater driven estuarine circulation is not the dominant mechanism for water mass renewal inside the fjord.

Along-shore Winds

12 hourly wind velocity (at 10 m) data are obtained from NASA's Quick Scatterometer (QuikSCAT; http://podaac.jpl.nasa.gov). Winds in the coastal region outside of Sermilik Fjord are derived by averaging across a region bounded by 36-39º W and 64.5-66º N (see Figure 3c). This region is large enough to ensure that data coverage is always available and minimizes the effect of data gaps that commonly occur in the proximity of the coast.

We note that the winds over the shelf have relatively large spatial coherence and that our results are not overly sensitive to the exact ‘region’ used for averaging. Positive along-shore winds are oriented at 54º (see Figure 3c). The wind-stress is obtained using the Large and Pond formulation[29] (Figure 4a and Supplementary Figure 2a). Wind events are defined as along-shore wind events whose magnitude exceeds 0.1 N m^{-2} and whose duration is longer than 1 day.

Intermediary Circulation

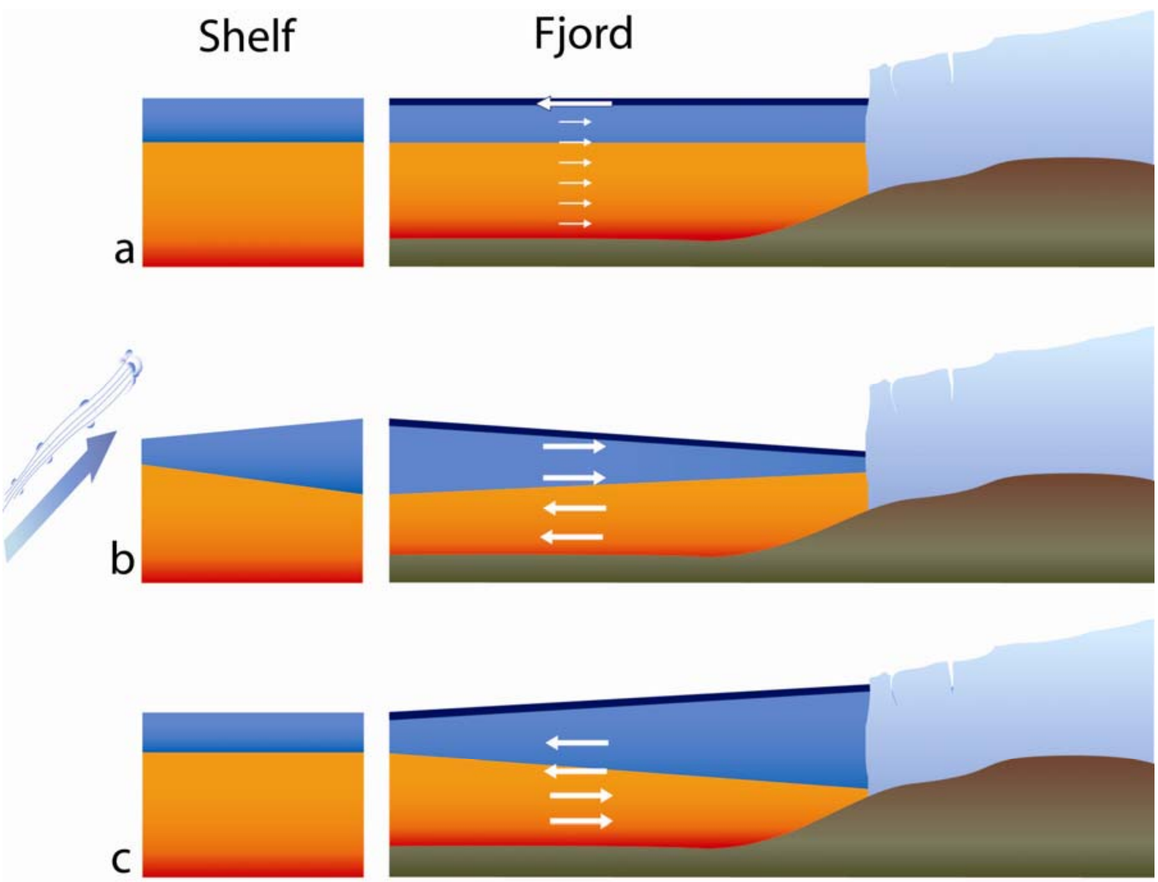

Supplemental Figure 1 Circulation in Sermilik Fjord a) Classic estuarine circulation in the absence of wind-forcing: a fast outflowing glacial meltwater plume and a weaker compensating inflow at depth. Wind-driven circulation: b) Northeasterly winds ‘pile-up’ water and depress the halocline at the mouth driving an inflow in the upper layer and outflow at depth. c) After the wind ceases and the shelf region returns to pre-event conditions and the fjord relaxes through the reverse circulation.

Analysis of the 8-month mooring record

The third mooring, carrying a single CTD recorder was deployed in early September 2008 and recovered in mid-August 2009 (see Methods Summary). Its initial location coincided with that of the shallow summer mooring but, after having been hit and displaced by ice several times, the mooring settled at 65 m at the end of December, 40 m deeper than its original depth. Spatially, the mooring was displaced less than 100 m from its original location. To remove any bias due to displacement, we restrict this analysis to data from December 28, 2008 to August 20, 2009 when the mooring remained at one location (and depth). Post-recovery calibrations did not show any sensor drift. The mooring recorded temperature (T), salinity (S) and pressure (P) every half hour throughout its deployment. These data were filtered with a 40 hour Hanning window to remove tidal and other high frequency noise (Supplementary Figure 2 b-d). To quantify the fjord’s response to along-shore wind events, which have time-scales on the order of several days, we removed long term variations (such as seasonal) from the records by subtracting a 30-day low-pass filtered time series (also using a 30-day Hanning window). The resulting time series of anomalies are shown in Supplementary Figure 2e. The along shore wind stress outside of the fjord for the same period is shown in Supplementary Figure 2a. An anomaly time series for the wind is obtained in the same way as for the ocean variables, Supplementary Figure 2e.

Visual inspection of the curves in Supplementary Figure 2 shows that positive wind stress anomalies are associated with positive pressure (equivalent to positive sea-surface height), negative salinity, and negative temperature anomalies. This is the expected response for a northeasterly wind event described in the text and Supplementary Figure 1 b and c. A simple regression of the anomaly time series for the fjord's properties on the wind stress anomaly time series reveals that all three are significantly correlated at the 99% level using 64 degrees of freedom (193 day long record with a 3-day decorrelation time scale), Supplementary Table 1. The correlation is largest for the pressure record which is representative of sea-surface height variability and at zero lag. (Mooring blow down is negligible given the length of the mooring, less than 1 m, and, also, it cannot account for negative pressure anomalies.) This is consistent with a rapid barotropic adjustment of the fjord. Maximum correlations with temperature and salinity are found at 1 day lag consistently with the slower baroclinic response.

Supplementary Table 1. Correlations of variables from the long mooring record with the alongshore wind stress.

Variable	R	Lag	Significant
Salinity	-0.33	1 day	$p < 0.01$
Temperature	-0.46	1 day	$p < 0.01$
Pressure	0.53	0	$p < 0.01$

Finally, it is evident from Supplementary Figure 2 that the wind-driven intermediary circulations do not account for all of the variability at this depth. Departures from this correlation are expected to occur and, we argue, are not inconsistent with the conclusions of this study – that the wind-driven intermediary circulation is the dominant but not the only forcing of the fjord’s variability. Indeed, the mooring discussed here is shallow enough that one cannot rule out the impact of local air-sea fluxes both during the wintertime period (as sea-ice forms in the fjord) and during the summer (when summer heating may be mixed down). The latter may explain the warming observed in late summer when there appear to be few or no wind-events. Second, and as noted in the main text, intermediary circulations will arise from any mechanism that generates a fjord/shelf pressure gradient (e.g. coastally trapped waves or eddies). Indeed on intermediary-circulation-like event occurs in mid-July but it is not associated with a wind-event (Supplementary Figure 2).

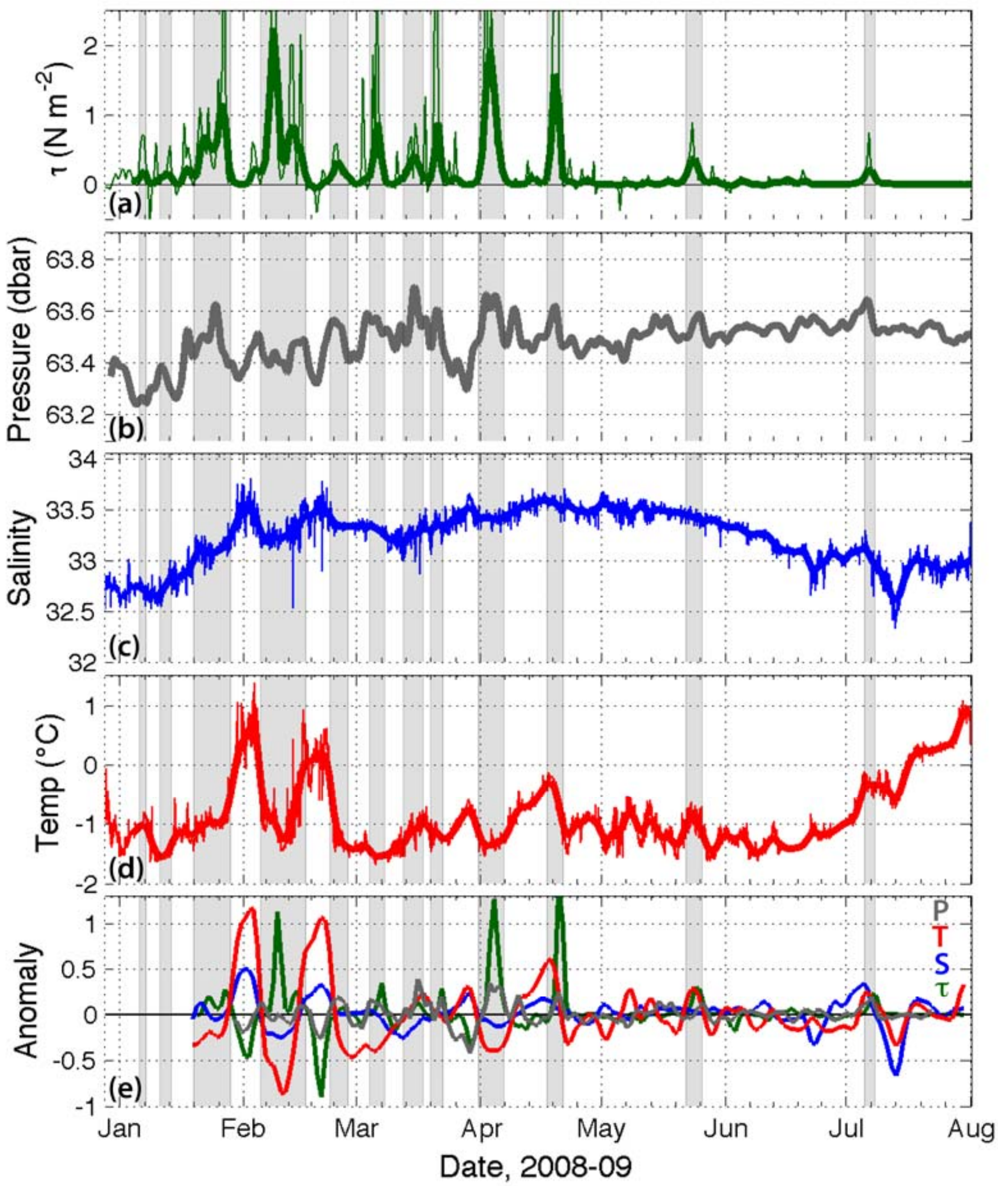

Supplementary Figure 2. (a) Time series of the alongcoast windstress, τ (N m^{-2}), outside Sermilik Fjord measured by the QuikSCAT scatterometer (see Supplementary Methods). The light line is the original data and the heavy line is the 40-hr low-passed time-series. Shading highlights downwelling ($\tau > 0$) wind. (b) The 40-hr low-pass filtered pressure record from the shallow mooring. (c) Same as in *b*, but for salinity. (d) Same as in *b*, but for temperature. (e) Time series of pressure (P), temperature (T), salinity (S), and wind stress (τ) anomalies. The wind stress and pressure anomalies have been shifted one day to correspond with the maximum correlations found with T and S. The τ, S, and P anomalies are scaled by a factor of 2 to help visualization. Units are the same as in panels a) to d).

28. Knauss, J. A. *Introduction to Physical Oceanography*. 2nd edition, Prentice-Hall, New Jersey, 309 pp (1997)

29. Large, W.G. & Pond, S. Open ocean momentum flux measurements in moderate to strong winds. *J. Phys. Oce*. **11**, 324-336 (1981)